Reversible ordering and disordering of the vortex lattice in UPt_3

K. E. Avers,[1,2,*] S. J. Kuhn,[3,†] A. W. D. Leishman,[3] W. J. Gannon,[1,‡] L. DeBeer-Schmitt,[4] C. D. Dewhurst,[5] D. Honecker,[5] R. Cubitt,[5] W. P. Halperin,[1] and M. R. Eskildsen[3,§]

[1]*Department of Physics and Astronomy, Northwestern University, Evanston, Illinois 60208, USA*
[2]*Center for Applied Physics & Superconducting Technologies, Northwestern University, Evanston, Illinois 60208, USA*
[3]*Department of Physics and Astronomy, University of Notre Dame, Notre Dame, Indiana 46556, USA*
[4]*Large Scale Structures Section, Neutron Scattering Division, Oak Ridge National Laboratory, Oak Ridge, Tennessee 37831, USA*
[5]*Institut Laue-Langevin, 71 avenue des Martyrs, CS 20156, F-38042 Grenoble cedex 9, France*

(Received 22 March 2021; revised 9 August 2021; accepted 6 May 2022; published 17 May 2022)

When studied by small-angle neutron scattering, the vortex lattice (VL) in UPt_3 undergoes a gradual disordering as a function of time due to ^{235}U fission. This temporarily heats regions of the sample above the critical temperature, where, upon recooling, the vortices remain in a quenched disordered state. The disordering rate is proportional to the magnetic field, suggesting that it is governed by collective VL properties such as the elastic moduli. An ordered VL can be re-formed by applying a small field oscillation, showing that the fission does not cause detectable radiation damage to the UPt_3 crystals, even after long exposure.

DOI: 10.1103/PhysRevB.105.184512

I. INTRODUCTION

Quantized vortices are introduced in a type-II superconductor subjected to an applied magnetic field [1]. Understanding and controlling vortex matter is of both fundamental interest and practical importance since vortex motion leads to dissipation. In an idealized scenario, vortices will arrange themselves in a perfectly ordered vortex lattice (VL) due to their mutual repulsion [2–4]. In reality, however, thermal effects and/or pinning to material defects is always present, and the balance between these competing factors determines the structural and dynamic properties of vortex matter [5–10]. This leads to a complex, high-dimensional phase diagram, where transitions between different states are driven not only by changes in intensive quantities, such as the field or temperature, but also by the amount of imperfection or impurities which affect the vortex pinning. An example of the latter is columnar defects introduced by heavy-ion irradiation [11]. In many applications, control of vortex dynamics is of critical importance such as for high coherence in superconducting radio frequency (rf) cavities used in accelerators [12] and for quantum information science [13].

The ability to manipulate the vortices experimentally is essential to the study of vortex matter. Frequently, the VL configuration will depend on the field and temperature history, either in the degree of ordering [14–16] or in the orientation of the VL relative to the crystalline axes of the host material [17–19]. In materials with weak vortex pinning, it is possible to anneal quenched disorder or dislodge the system from an ordered but metastable configuration by temporarily exciting the VL, either by applying a transport current [20–24] or by applying a small-amplitude magnetic field oscillation [25–27]. This causes vortex motion and "shakes" them free of local minima in their collective energy landscape. In contrast, vortex matter in superconductors with strong pinning often become more disordered following a vortex shaking [28–30].

Here, we demonstrate an approach to structural studies of vortex matter whereby reversible quenched disorder can be introduced locally without permanently affecting the host superconducting material. Specifically, we used small-angle neutron scattering (SANS) to study the VL in the topological superconductor UPt_3, which undergoes a gradual disordering on a time scale of tens of minutes as it is subjected to a beam of cold neutrons. The disordering is due to local heating events caused by neutron-induced fission of ^{235}U, which leaves an increasing fraction of the sample occupied by a disordered vortex configuration. While the system does not spontaneously reorder once the local heating has been dissipated, it is possible to reanneal the VL by the application of a damped field oscillation.

II. EXPERIMENTAL DETAILS

The SANS measurements [31] were performed on the CG-2 General Purpose SANS instrument at the High Flux Isotope Reactor at Oak Ridge National Laboratory (ORNL) [32] and on the D33 instrument at the Institut Laue-Langevin (ILL) [33–35], using a fixed neutron wavelength obtained by a velocity selector. Two high-quality single crystals were studied, designated ZR8 and ZR11, both of which have been used in previous SANS measurements [36–38]. The characteristics of

*Present address: Department of Physics, University of Maryland, College Park, Maryland 20742, USA.
†Present address: Center for Exploration of Energy & Matter, Indiana University, Bloomington, Indiana 47408, USA.
‡Present address: Department of Physics and Astronomy, University of Kentucky, Lexington, Kentucky 40506, USA.
§eskildsen@nd.edu

 ©2022 American Physical Society

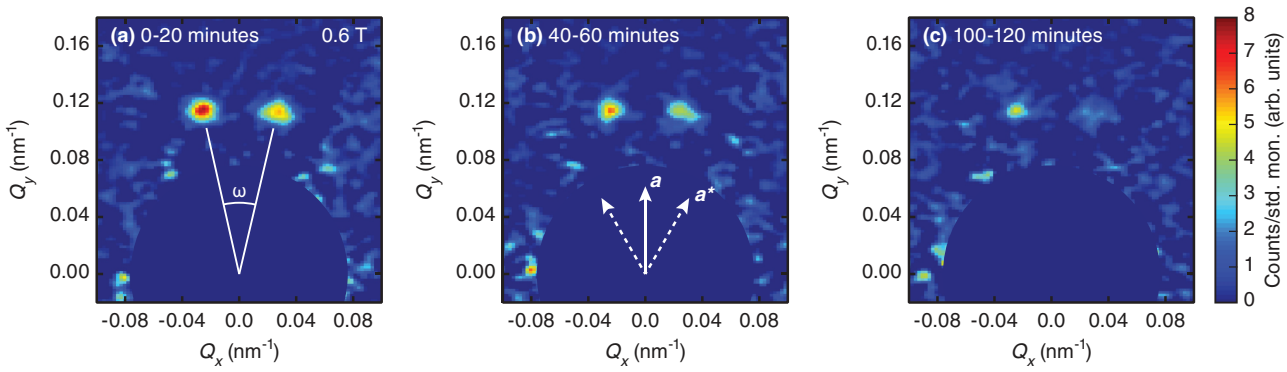

FIG. 1. Diffraction patterns obtained on ZR11 at 0.6 T (ORNL), measured at different times following the preparation of a pristine VL and without the application of periodic field oscillations. Each diffraction pattern was counted for 20 min and uses the same color scale. The peak splitting is indicated in (a), and crystallographic directions within the scattering plane are indicated in (b). Only peaks at the top of the detector satisfied the Bragg condition. Background scattering is subtracted, and the detector center near $Q = 0$ is masked off. The intensity is normalized to the standard monitor (std. mon.).

each crystal are given in the Supplemental Material [39]. Unless otherwise stated, SANS measurements were carried out in a "rocked on" configuration, satisfying the Bragg condition for VL peaks at the top of the two-dimensional position-sensitive detector, as seen in Fig. 1. Measurements were performed using a dilution refrigerator operating at a base temperature of 50–65 mK $\sim 0.1T_c$ and with applied magnetic fields between 0.3 and 1.0 T applied along the crystalline **c** axis. Background measurements, obtained either in zero field or above the upper critical field, were subtracted from the foreground data.

Prior to each SANS measurement sequence a pristine VL was prepared by applying a damped magnetic field oscillation with an initial amplitude of 20 mT around the measurement field. This was previously found to produce a well-ordered VL with a homogeneous vortex density [37]. In addition, a ±5-mT oscillation was applied periodically during some of the SANS measurements to maintain an ordered VL [37]. All field oscillations end with a reduction in the magnetic field magnitude, corresponding to a decrease of the vortex density.

III. RESULTS

Figure 1 shows SANS VL diffraction patterns illustrating the main result of this paper. In all instances a pair of Bragg peaks are observed, split by an angle ω around the crystalline **a** axis as indicated in Fig. 1(a). A total of six such pairs exist, but to conserve beam time only the peaks at the top of the detector were brought into the Bragg condition. The split peaks correspond to VL domains rotated about the crystalline **c** axis in a clockwise or counterclockwise direction, with the intensity difference being due to an unequal domain population [37,38]. All diffraction patterns in Fig. 1 were recorded at the same temperature and magnetic field and in the absence of a periodic field oscillation, and show a clear reduction in the intensity as a function of time. This reflects a gradual VL disordering and a corresponding broadening of the Bragg peaks in reciprocal space. Although the poor resolution within the detector plane makes the broadening difficult to resolve [31], it is clearly seen in the VL rocking curves discussed later. Note that what is characterized as an ordered VL is most likely a Bragg glass phase with algebraically decaying correlations [7,8,40–44], although it is not possible to establish this conclusively from the present SANS data.

To verify that the VL disordering is due to the neutron beam, measurements were performed both during a continuous exposure and following a prolonged period with the beam turned off. These are summarized in Fig. 2. Prior to the measurements a pristine VL was prepared, and the first data point (0–20 min) was collected while a ±5-mT field oscillation was performed roughly every 60 s to maintain an ordered VL. The neutron shutter was then closed, and the periodic field oscillation was turned off. After 90 min the shutter was reopened, and four subsequent 15-min measurements of the VL intensity were made. The shutter was then closed again, and a ±5-mT field oscillation was applied to reanneal the VL. After an additional 2 h, the shutter was opened for a final 15-min measurement.

The data in Fig. 2 establish conclusively that the VL disordering occurs when the sample is illuminated by the neutron

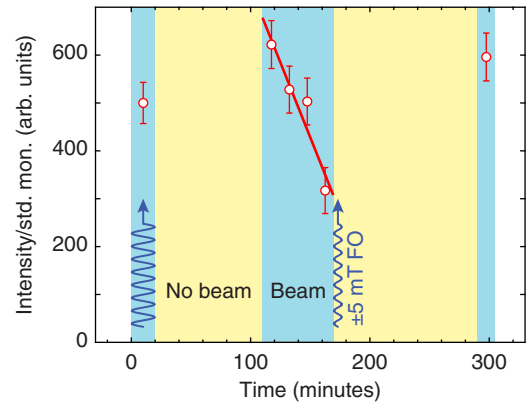

FIG. 2. Exposure test on ZR11 at 0.8 T (ORNL), where blue (yellow) shading indicates when the neutron beam was on (off). The VL scattered intensity is normalized to the standard monitor count. Field oscillations (FO) of ±5 mT were applied periodically during the first 20-min measurement and at 170 min after the neutron beam was shut off.

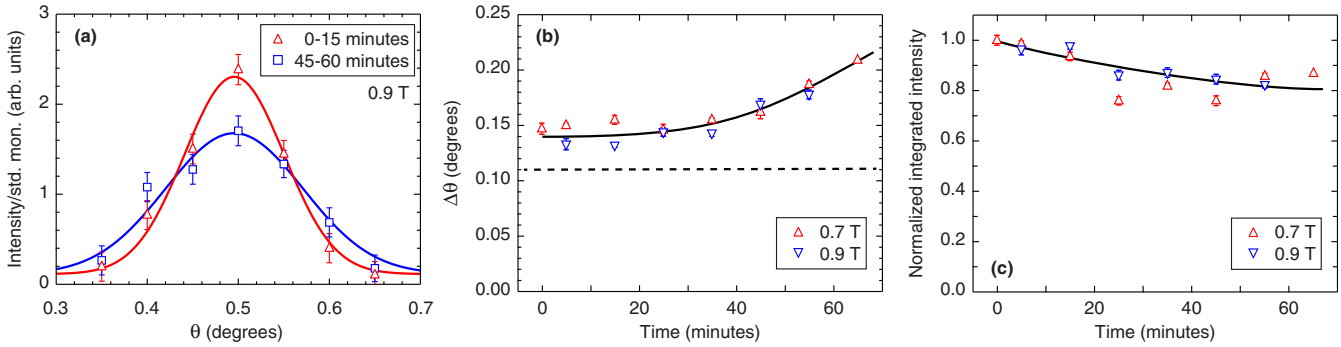

FIG. 3. (a) Rocking curves obtained on ZR8 at 0.9 T (ILL), measured during the first 15 min after the preparation of a pristine VL and after 45–60 min. Curves are Gaussian fits to the data as described in the text. (b) Time dependence of the fitted rocking curve width. The dashed line indicates the experimental resolution. (c) Time dependence of the fitted integrated intensity, normalized to the value for the pristine VL. Solid lines in (b) and (c) are guides to the eye.

beam, and is attributed to ^{235}U fission events in the sample. Specifically, the intensity decreases to roughly half its initial value between 110 and 170 min, while no reduction is observed during the two periods where the beam was off. Figure 2 also confirms that an ordered VL is achieved by the application of the damped field oscillation, indicated by the recovery of the intensity both in the second and in the final data point. Finally, the intensity measured after the shutter opening at 110 and 290 min is somewhat higher than for the first data point. This is ascribed to the prolonged absence of fission heating of the UPt_3 crystals resulting in a lower overall sample temperature (see Supplemental Material). The possibility of a spontaneous reordering of the VL was also investigated. After 1 h without beam exposure the intensity of a disordered VL was found to increase only modestly, with a count rate within measurement error of that recorded immediately before the beam was turned off. Again, the slight increase is likely due to a lower sample temperature, and any reordering thus occurs on time scales much longer than the beam-induced disordering if at all.

We now return to the broadening of the VL reflections perpendicular to the detector plane. Figure 3(a) shows rocking curves of the scattered intensity at 0.9 T as the split VL peak is rotated through the Bragg condition, where θ is the angle between the magnetic field and the neutron beam direction. An increase in the width and a reduction in the maximum intensity at $\theta \approx 0.5^\circ$ are clearly observed at the later time, consistent with Figs. 1 and 2, which were measured at the peak of the rocking curve. The rocking curves are fitted to a Gaussian

$$I(\theta) = \frac{I_{\mathrm{VL}}}{\Delta\theta}\ \exp\left[-2\ln(4)\left(\frac{\theta-\theta_0}{\Delta\theta}\right)^2\right], \qquad (1)$$

where I_{VL} is proportional to the integrated intensity, θ_0 is the peak position, and $\Delta\theta$ is the full width at half maximum (FWHM). Fitted values of $\Delta\theta$ and I_{VL} as a function of time are shown in Figs. 3(b) and 3(c), respectively, for fields of 0.7 and 0.9 T. The integrated intensity is normalized to the value for the pristine VL, obtained either from measurements performed in the presence of a periodic ±5-mT field oscillation (0.7 T) or by a linear extrapolation of I_{VL} to zero time (0.9 T).

The rocking curve width increases with time for both measured fields as seen in Fig. 3(b), confirming the gradual VL disordering hypothesized earlier. At shorter times, $\Delta\theta$ approaches the experimental resolution estimated by

$$\Delta\theta_{\mathrm{res}} = \sqrt{\delta\theta^2 + \left(\frac{q_{\mathrm{VL}}\lambda_{\mathrm{n}}}{2\pi}\frac{\Delta\lambda_{\mathrm{n}}}{\lambda_{\mathrm{n}}}\right)^2}, \qquad (2)$$

where $\delta\theta$ is the standard deviation of the beam divergence, $\lambda_{\mathrm{n}} = 0.75$ nm is the neutron wavelength, and $\Delta\lambda_{\mathrm{n}}/\lambda_{\mathrm{n}} = 15\%$ (ORNL) or 10% (ILL) is the FWHM wavelength spread [45]. The VL scattering vector $q_{\mathrm{VL}} = 2\pi(2B/\sqrt{3}\phi_0)^{1/2}$, where $\phi_0 = 2068$ T nm^2 is the flux quantum. The near-constant value of $\Delta\theta$ during the first roughly 30 min indicates an intrinsic VL Bragg peak width which is much smaller than $\Delta\theta_{\mathrm{res}}$, with a clear broadening observed only once the two become comparable. The reciprocal rocking curve width (in radians) can thus be taken as a lower bound on the longitudinal VL correlation length, $\zeta_L \geqslant 2(q_{\mathrm{VL}}\,\Delta\theta)^{-1} \approx 6$–$7\ \mu$m. The absence of a time lag in the reduction in the integrated intensity in Fig. 3(c) provides further evidence that the VL disordering begins as soon as the sample is subjected to the neutron beam. Here, I_{VL} decreases by ∼20% within the first hour, possibly leveling off at the longer times. The decrease in I_{VL} indicates a disruption of the VL, and possibly an evolution towards a vortex glass phase [44]. Notably, the 0.9-T measurements were not preceded by a beam-off period, and the reduction in I_{VL} is thus not due to a gradual heating of the sample.

To quantify the VL disordering, measurements of the rocking curve peak intensity as a function of neutron exposure were performed for a range of magnetic fields. Figure 4(a) shows examples of decay curves for three different fields versus the number of absorbed neutrons, demonstrating that the VL is disordered more quickly at higher magnetic fields. The disordering rates, defined by the slope of linear fits to the data, are summarized in Fig. 4(b) for all measurement sequences and both UPt_3 crystals. Here, the rates are normalized to absorbed neutrons per unit volume to allow for a direct comparison of the ZR8 and ZR11 samples (see Supplemental Material).

While the decreasing intensity in Fig. 4(a) could in principle be due to a gradual heating of the sample, several factors allow us to rule this out. These include the constant

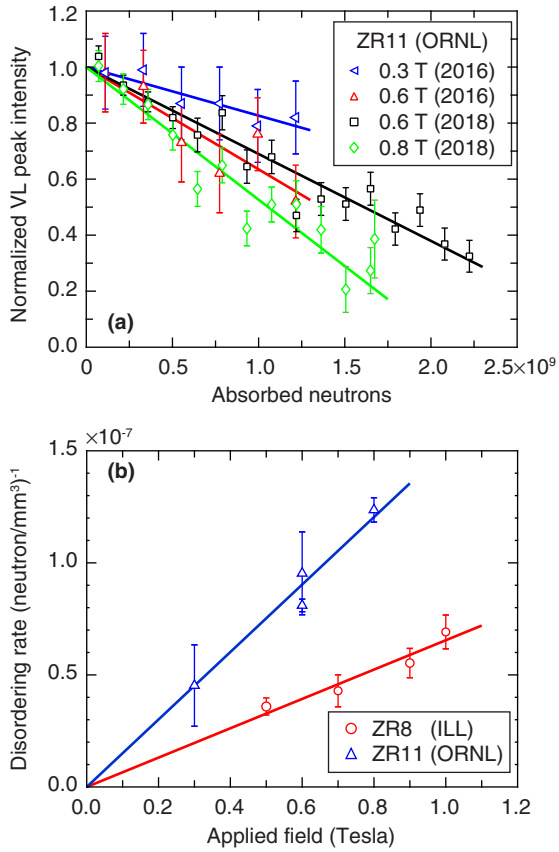

FIG. 4. (a) VL scattering rate vs absorbed neutrons per area transmitted through the sample for different fields. Data were obtained on ZR11 at ORNL during separate experiments (2016 and 2018). Intensities are normalized such that linear fits (solid lines) extrapolate to unity for the pristine VL. (b) Disordering rate per unit volume vs magnetic field for both UPt_3 samples. Lines are linear fits to the ZR8 and ZR11 data, constrained to pass through the origin.

VL splitting in Fig. 1, which is in contrast to the rapid decrease observed with increasing temperature [38]. Furthermore, successive measurements at 0.6 T, separated only by the application of a damped field oscillation, show the same decay of the VL intensity (see Supplemental Material).

IV. DISCUSSION

A strong temperature history dependence of the UPt_3 VL is well documented. For example, the ability to thermally quench the VL in UPt_3 was used to facilitate SANS studies of the superconducting A phase which exists just below T_c [17]. Here, VL Bragg peaks were observed oriented along or split around the crystalline $\boldsymbol{a}$ axis, depending on the quench temperature. In comparison, a slow cooling from temperatures above T_c leads to a different VL configuration, with Bragg peaks along the $\boldsymbol{a}^*$ axis. We do not observe any VL scattering around $\boldsymbol{a}^*$, either in the rocked-on measurements or in the rocking curves in Fig. 3 which would satisfy the Bragg condition for peaks at this location. The vanishing scattering in our SANS measurements is therefore not due to intensity being transferred from one VL peak to another.

We propose that the observed decreasing intensity with increasing neutron exposure arises from a rapid thermal cycling, due to fission events which locally heat the sample above the critical temperature. Following the thermal transient, vortices re-form in a disordered configuration due to the quench through the vortex glass state below the superconducting transition [5,44]. Support for such a scenario comes from SANS studies of $NbSe_2$, where the degree of VL ordering was found to depend sensitively on the thermal history in the vicinity of the so-called peak effect in the critical current [15,16,46]. The peak effect is associated with the order-disorder transition between the vortex glass and Bragg glass states [47,48] and is also observed in UPt_3 [49].

The volume affected by a single fission event may be estimated from the low-temperature specific heat ($C/T \approx 1.6T$ J K^{-3} mol^{-1}) and the mass density ($\rho = 19.4$ g/cm^3) of UPt_3 [50], yielding a sphere of diameter $\sim$34 μm heated above T_c. This should be considered an order-of-magnitude estimate since it assumes the applicability of the equilibrium specific heat during the fission process and ignores both the field dependence of the specific heat [51] and the thermal conductivity [52]. The size of the affected volume exceeds the 4–6-μm range of the Ba and Kr fission products in UPt_3 [53]. It is also much greater than the vortex spacing given by $a_0 = (2\phi_0/\sqrt{3}B)^{1/2}$, with the diameter obtained above corresponding to approximately $400a_0$ to $700a_0$ as the field is increased from 0.3 to 1 T. A single fission event thus affects large sections of the VL, several times greater than the longitudinal correlation length estimated from the rocking curves.

A detailed understanding of the fission-induced VL disordering will require a careful analysis and is outside the scope of this paper. Nevertheless, two important points may be deduced from Fig. 4(b). First, for each UPt_3 crystal the disordering rate is directly proportional to the applied magnetic field, indicating that it is governed by VL properties. Here, the elastic moduli, which increase with rising vortex density [6], will be important to consider as a greater stiffness will allow VL "shock waves" to propagate farther from the volume directly affected by the fission events. Second, the ratio of the disordering rate to the applied field differs for ZR8 and ZR11. The latter crystal is of higher quality (see Supplemental Material) and therefore expected to exhibit less vortex pinning. This will make the ZR11 VL less resilient against disordering, as disruptions can more easily propagate away from the volume directly affected by the fission event. As stacking faults are the principal crystalline defects in UPt_3 [54] and directly visible in the small-angle background scattering [17], the relation between the disordering rate and sample quality should be quantified in future SANS experiments.

A remaining question is, How, and to what degree, are the UPt_3 crystals affected by the fission processes? The incorporation of fissionable elements and subsequent irradiation by neutrons has previously been used to create defects and enhance the vortex pinning in conventional superconductors as well as high-T_c oxides [55–57]. Here, an increase in the critical current was found for fission event densities of the order of 10^{14}–10^{15} cm^{-3}. In comparison, the UPt_3 ZR8 crystal has experienced $\sim 10^{11}$ fission events during the roughly 1 month of accumulated irradiation. It is therefore not surprising that the intrinsic vortex pinning has not increased sufficiently

to affect the SANS measurements, as it is still possible to achieve an ordered VL by a field oscillation.

Before concluding, we also consider how the fission events affect the superconducting order parameter in UPt_3 and our recent SANS experiments, which provide direct evidence for broken time-reversal symmetry in the B phase [37]. Here, differences in the VL orientation relative to the crystalline axes were observed between states with the Cooper pair orbital angular momentum either parallel or antiparallel to the applied magnetic field. The latter corresponds to a metastable order parameter configuration, achieved by reducing the magnetic field at low temperature to enter the B phase and establish the chiral direction, eventually passing through zero and thus reversing the field direction. Fission events could potentially impact the chiral direction in the regions temporarily heated above T_c and, if this direction is reversed upon recooling, lead to the formation of order parameter domain boundaries.

Based on the rate and affected volume, the fraction of the sample that remains unaffected by fission will decrease exponentially with a time constant of approximately 6 min. This is much shorter than the SANS count times which, at the higher fields, reach several hours. Since a difference in the VL was indeed observed between the two order parameter configurations [37], a fission-induced reversal of the chiral direction, and the accompanying order parameter domain formation, does not appear to take place. This is consistent with both tunneling [58] and Kerr rotation [59] measurements, showing an absence of order parameter domain formation in UPt_3 even in the absence of a training field, and suggesting that a single order parameter domain spans the entire crystal [59]. Using the roughly 1 mm length scale associated with these experiments as a lower limit on the domain size yields a volume much greater than that affected by a fission event. This implies that domain formation in UPt_3 is energetically unfavorable and supports our conclusion that the order parameter in the SANS measurements is re-formed with the same chiral direction as the surrounding sample.

V. CONCLUSION

In summary, we have shown that the VL in UPt_3 undergoes a gradual fission-induced disordering when exposed to a beam of cold neutrons. Fission events heat regions of the sample above T_c, which upon recooling host a quenched vortex glass state. The disordering rate is proportional to the vortex density, suggesting that it is governed by the VL stiffness. Our observations provide possibilities for studies of vortex matter whereby local and reversible disorder can be combined with, e.g., thermal disordering. We also speculate that the magnitude of field oscillation required for maintaining an ordered VL will be less than that needed to reorder a disordered VL, due to the different structural properties. Finally, the use of periodic field oscillations to mitigate the VL disordering can be applied to other U-containing superconductors where SANS studies have to date been unsuccessful.

ACKNOWLEDGMENTS

We are grateful to J. A. Sauls for numerous discussions over the years and to U. Köster for providing estimates of the sample heating due to fission. This work was supported by the US Department of Energy, Office of Basic Energy Sciences, under Awards No. DE-SC0005051 (M.R.E., University of Notre Dame; neutron scattering) and No. DE-FG02-05ER46248 (W.P.H., Northwestern University; crystal growth and neutron scattering). A portion of this research used resources at the High Flux Isotope Reactor, a DOE Office of Science User Facility operated by the Oak Ridge National Laboratory. Part of this work is based on experiments performed at the Institut Laue-Langevin, Grenoble, France.

[1] R. P. Huebener, *Magnetic Flux Structures in Superconductors* (Springer, New York, 2001).
[2] A. A. Abrikosov, Sov. Phys. JETP **5**, 1174 (1957).
[3] W. H. Kleiner, S. H. Autler, and L. M. Roth, Phys. Rev. **133**, A1226 (1964).
[4] J. Matricon, Phys. Lett. **9**, 289 (1964).
[5] G. Blatter, M. V. Feigel'man, V. B. Geshkenbein, A. I. Larkin, and V. M. Vinokur, Rev. Mod. Phys. **66**, 1125 (1994).
[6] E. H. Brandt, Rep. Prog. Phys. **58**, 1465 (1995).
[7] T. Giamarchi and P. Le Doussal, Phys. Rev. B **52**, 1242 (1995).
[8] T. Giamarchi and P. Le Doussal, Phys. Rev. B **55**, 6577 (1997).
[9] T. Nattermann and S. Scheidl, Adv. Phys. **49**, 607 (2000).
[10] P. Le Doussal, Int. J. Mod. Phys. B **24**, 3855 (2010).
[11] M. Menghini, Y. Fasano, F. de la Cruz, S. S. Banerjee, Y. Myasoedov, E. Zeldov, C. J. van der Beek, M. Konczykowski, and T. Tamegai, Phys. Rev. Lett. **90**, 147001 (2003).
[12] M. Checchin and A. Grassellino, Phys. Rev. Applied **14**, 044018 (2020).
[13] A. Romanenko, R. Pilipenko, S. Zorzetti, D. Frolov, M. Awida, S. Belomestnykh, S. Posen, and A. Grassellino, Phys. Rev. Applied **13**, 034032 (2020).
[14] Z. L. Xiao, O. Dogru, E. Y. Andrei, P. Shuk, and M. Greenblatt, Phys. Rev. Lett. **92**, 227004 (2004).
[15] M. Marziali Bermudez, M. R. Eskildsen, M. Bartkowiak, G. Nagy, V. Bekeris, and G. Pasquini, Phys. Rev. Lett. **115**, 067001 (2015).
[16] M. Marziali Bermudez, E. R. Louden, M. R. Eskildsen, C. D. Dewhurst, V. Bekeris, and G. Pasquini, Phys. Rev. B **95**, 104505 (2017).
[17] A. Huxley, P. Rodière, D. M. Paul, N. van Dijk, R. Cubitt, and J. Flouquet, Nature (London) **406**, 160 (2000).
[18] P. Das, C. Rastovski, T. R. O'Brien, K. J. Schlesinger, C. D. Dewhurst, L. DeBeer-Schmitt, N. D. Zhigadlo, J. Karpinski, and M. R. Eskildsen, Phys. Rev. Lett. **108**, 167001 (2012).
[19] S. Okuma, D. Shimamoto, and N. Kokubo, Phys. Rev. B **85**, 064508 (2012).
[20] U. Yaron, P. L. Gammel, D. A. Huse, R. N. Kleiman, C. S. Oglesby, E. Bucher, B. Batlogg, D. J. Bishop, K. Mortensen, K. Clausen, C. A. Bolle, and F. De La Cruz, Phys. Rev. Lett. **73**, 2748 (1994).
[21] U. Yaron, P. L. Gammel, D. A. Huse, R. N. Kleiman, C. S. Oglesby, E. Bucher, B. Batlogg, D. J. Bishop, K. Mortensen, and K. N. Clausen, Nature (London) **376**, 753 (1995).

[22] A. Duarte, E. Fernandez Righi, C. A. Bolle, F. de la Cruz, P. L. Gammel, C. S. Oglesby, E. Bucher, B. Batlogg, and D. J. Bishop, Phys. Rev. B **53**, 11336 (1996).

[23] A. Pautrat, J. Scola, C. Simon, P. Mathieu, A. Brûlet, C. Goupil, M. J. Higgins, and S. Bhattacharya, Phys. Rev. B **71**, 064517 (2005).

[24] G. Li, E. Y. Andrei, Z. L. Xiao, P. Shuk, and M. Greenblatt, Phys. Rev. Lett. **96**, 017009 (2006).

[25] S. J. Levett, C. D. Dewhurst, and D. M. Paul, Phys. Rev. B **66**, 014515 (2002).

[26] E. R. Louden, C. Rastovski, S. J. Kuhn, A. W. D. Leishman, L. DeBeer-Schmitt, C. D. Dewhurst, N. D. Zhigadlo, and M. R. Eskildsen, Phys. Rev. B **99**, 060502(R) (2019).

[27] E. R. Louden, C. Rastovski, L. DeBeer-Schmitt, C. D. Dewhurst, N. D. Zhigadlo, and M. R. Eskildsen, Phys. Rev. B **99**, 144515 (2019).

[28] M. R. Eskildsen, L. Y. Vinnikov, T. D. Blasius, I. S. Veshchunov, T. M. Artemova, J. M. Densmore, C. D. Dewhurst, N. Ni, A. Kreyssig, S. L. Bud'ko, P. C. Canfield, and A. I. Goldman, Phys. Rev. B **79**, 100501(R) (2009).

[29] D. S. Inosov, T. Shapoval, V. Neu, U. Wolff, J. S. White, S. Haindl, J. T. Park, D. L. Sun, C. T. Lin, E. M. Forgan, M. S. Viazovska, J. H. Kim, M. Laver, K. Nenkov, O. Khvostikova, S. Kuhnemann, and V. Hinkov, Phys. Rev. B **81**, 014513 (2010).

[30] D. S. Inosov, J. S. White, D. V. Evtushinsky, I. V. Morozov, A. Cameron, U. Stockert, V. B. Zabolotnyy, T. K. Kim, A. A. Kordyuk, S. V. Borisenko, E. M. Forgan, R. Klingeler, J. T. Park, S. Wurmehl, A. N. Vasiliev, G. Behr, C. D. Dewhurst, and V. Hinkov, Phys. Rev. Lett. **104**, 187001 (2010).

[31] S. Mühlbauer, D. Honecker, E. A. Périgo, F. Bergner, S. Disch, A. Heinemann, S. Erokhin, D. Berkov, C. Leighton, M. R. Eskildsen, and A. Michels, Rev. Mod. Phys **91**, 015004 (2019).

[32] W. T. Heller, M. Cuneo, L. Debeer-Schmitt, C. Do, L. He, L. Heroux, K. Littrell, S. V. Pingali, S. Qian, C. Stanley, V. S. Urban, B. Wu, and W. Bras, J. Appl. Crystallogr. **51**, 242 (2018).

[33] C. D. Dewhurst, J. Appl. Crystallogr. **47**, 1180 (2014).

[34] M. R. Eskildsen, K. Avers, C. Dewhurst, W. Gannon, W. P. Halperin, S. Kuhn, and J. White, Chiral effects on the vortex lattice in UPt_3, Institut Laue-Langevin, 2016, doi:10.5291/ILL-DATA.5-42-402.

[35] M. R. Eskildsen, K. Avers, C. Dewhurst, D. Honecker, A. Leishman, and J. White, Chiral effects on the vortex lattice in UPt_3, Institut Laue-Langevin, 2018, doi:10.5291/ILL-DATA.5-42-467.

[36] W. J. Gannon, W. P. Halperin, C. Rastovski, K. J. Schlesinger, J. Hlevyack, M. R. Eskildsen, A. B. Vorontsov, J. Gavilano, U. Gasser, and G. Nagy, New J. Phys. **17**, 023041 (2015).

[37] K. E. Avers, W. J. Gannon, S. J. Kuhn, W. P. Halperin, J. A. Sauls, L. DeBeer-Schmitt, C. D. Dewhurst, J. Gavilano, G. Nagy, U. Gasser, and M. R. Eskildsen, Nat. Phys. **16**, 531 (2020).

[38] K. E. Avers, W. J. Gannon, A. W. D. Leishman, L. DeBeer-Schmitt, W. P. Halperin, and M. R. Eskildsen, Front. Electron. Mater. **2**, 878308 (2022).

[39] See Supplemental Material at http://link.aps.org/supplemental/10.1103/PhysRevB.105.184512 for the characterization of the single crystals used for the SANS experiments, neutron absorption by the samples, estimate of the fission rate, and sample thermalization.

[40] R. Cubitt, E. M. Forgan, G. Yang, S. L. Lee, D. M. Paul, H. A. Mook, M. Yethiraj, P. H. Kes, T. W. Li, A. A. Menovsky, Z. Tarnawski, and K. Mortensen, Nature (London) **365**, 407 (1993).

[41] T. Klein, I. Joumard, S. Blanchard, J. Marcus, R. Cubitt, T. Giamarchi, and P. Le Doussal, Nature (London) **413**, 404 (2001).

[42] U. Divakar, A. J. Drew, S. L. Lee, R. Gilardi, J. Mesot, F. Y. Ogrin, D. Charalambous, E. M. Forgan, G. I. Menon, N. Momono, M. Oda, C. D. Dewhurst, and C. Baines, Phys. Rev. Lett. **92**, 237004 (2004).

[43] M. Laver, E. M. Forgan, A. B. Abrahamsen, C. Bowell, T. Geue, and R. Cubitt, Phys. Rev. Lett. **100**, 107001 (2008).

[44] R. Toft-Petersen, A. B. Abrahamsen, S. Balog, L. Porcar, and M. Laver, Nat. Commun. **9**, 901 (2018).

[45] J. S. Pedersen, D. Posselt, and K. Mortensen, J. Appl. Crystallogr. **23**, 321 (1990).

[46] N. D. Daniilidis, S. R. Park, I. K. Dimitrov, J. W. Lynn, and X. S. Ling, Phys. Rev. Lett. **99**, 147007 (2007).

[47] P. L. Gammel, U. Yaron, A. P. Ramirez, D. J. Bishop, A. M. Chang, R. Ruel, L. N. Pfeiffer, E. Bucher, G. D'Anna, D. A. Huse, K. Mortensen, M. R. Eskildsen, and P. H. Kes, Phys. Rev. Lett. **80**, 833 (1998).

[48] I. Joumard, J. Marcus, T. Klein, and R. Cubitt, Phys. Rev. Lett. **82**, 4930 (1999).

[49] U. Yaron, P. L. Gammel, G. S. Boebinger, G. Aeppli, P. Schiffer, E. Bucher, D. J. Bishop, C. Broholm, and K. Mortensen, Phys. Rev. Lett. **78**, 3185 (1997).

[50] R. Joynt and L. Taillefer, Rev. Mod. Phys. **74**, 235 (2002).

[51] A. P. Ramirez, N. Stücheli, and E. Bucher, Phys. Rev. Lett. **74**, 1218 (1995).

[52] H. Suderow, J. P. Brison, A. Huxley, and J. Flouquet, J. Low Temp. Phys. **108**, 11 (1997).

[53] Estimated using SRIM software package, http://www.srim.org.

[54] J.-I. Hong, Ph.D. thesis, Northwestern University, 1999.

[55] C. P. Bean, R. L. Fleischer, P. S. Swartz, and H. R. Hart Jr, J. Appl. Phys. (Melville, NY) **37**, 2218 (1966).

[56] R. L. Fleischer, H. R. Hart, K. W. Lay, and F. E. Luborsky, Phys. Rev. B **40**, 2163 (1989).

[57] L. Shan, H.-H. Wen, and S. X. Dou, Phys. C (Amsterdam) **390**, 80 (2003).

[58] J. D. Strand, D. J. Van Harlingen, J. B. Kycia, and W. P. Halperin, Phys. Rev. Lett. **103**, 197002 (2009).

[59] E. R. Schemm, W. J. Gannon, C. M. Wishne, W. P. Halperin, and A. Kapitulnik, Science **345**, 190 (2014).